I&EC research
Industrial & Engineering Chemistry Research

ARTICLE

pubs.acs.org/IECR

Hydrodynamic Cavitation as an Advanced Oxidation Technique for the Degradation of Acid Red 88 Dye

Virendra Kumar Saharan,[†] Aniruddha B. Pandit,[†,*] Panneer Selvam Satish Kumar,[‡] and Sambandam Anandan[‡]

[†]Chemical Engineering Department, Institute of Chemical Technology, Mumbai 400019, India

[‡]Nanomaterials & Solar Energy Conversion Lab, Department of Chemistry, National Institute of Technology, Trichy 620 015, India

ABSTRACT: In the present work, degradation of Acid Red 88 dye (AR88) has been carried out using one of the advanced oxidation processes, namely hydrodynamic cavitation (HC). The effect of various operating parameters such as inlet pressure, initial concentration of dye, pH of solution, addition of H_2O_2, and a catalyst ($Fe-TiO_2$) on the extent of decolorization and mineralization have been studied with the aim of maximizing the extent of degradation. The degradation of AR88 was found to follow first order kinetics under the condition examined. The study revealed that the extent of degradation increased with an increase in the initial dye concentration and the rate of degradation was found to be dependent on the solution pH. The degradation of AR88 is enhanced with the addition of H_2O_2 and catalyst ($Fe-TiO_2$). The comparative study of hydrodynamic cavitation and acoustic cavitation suggested that hydrodynamic cavitation is more energy efficient and gives higher degradation as compared to acoustic cavitation for equivalent power/energy dissipation. To observe the complete mineralization of the dye molecule, the total organic carbon (TOC) content was also measured at optimized condition for different experimental sets.

1. INTRODUCTION

The main source for water pollution is the industrial wastewater which contains large amounts of organic compounds such as textile dyes, aromatic compounds, chlorinated hydrocarbons, and phenolic compounds. These organic molecules are biorefractory or toxic to the micro-organisms. Hence, conventional biological processes are not able to completely degrade these compounds. Therefore, new technologies named as advanced oxidation processes (AOPs) have been explored by many researchers in the past few years. Advanced oxidation process (AOP) can be defined as the process that involves formation and subsequent attack of highly reactive free radicals such as $OH^{\bullet}$, $O^{\bullet}$ and $HOO^{\bullet}$, which are capable of oxidizing organic compounds. These processes include cavitation (mainly acoustic and hydrodynamic cavitation),[1−4] photocatalytic oxidation (using UV light/sunlight in the presence of semiconductor catalyst),[5−7] Fenton chemistry (using reaction between Fe ions and hydrogen peroxide),[8] and chemical oxidation (use of ozone and hydrogen peroxide).[9−11]

Most of these AOP techniques have been examined successfully on the laboratory scale but they are difficult to scale up on an industrial scale. Among these techniques cavitational reactors are novel and are the simplest to design and operate. Cavitation is defined as the formation, growth, and subsequent collapse of the cavities occurring in an extremely small interval of time (milliseconds), releasing large magnitudes of energy. The effects of cavity collapse are the creation of hot spots, the release of highly reactive free radicals, solid surface cleansing, and enhancement in mass transfer rates. The collapse of bubbles generates localized "hot spots" with transient temperatures of about 10000 K and pressures of about 1000 atm.[12] Under such extreme conditions water molecules are dissociated into OH and H radicals. These radicals then diffuse into the bulk liquid medium where they react with organic pollutants and oxidize them.

The two main mechanisms for the destruction of organic pollutants using cavitation are (1) the thermal decomposition/pyrolysis of the volatile pollutant molecule entrapped inside the cavity[13,14] and (2) the reaction of OH radicals with the pollutants.[15,16]

Cavitation is classified into four types based on the method of production of cavities, namely, acoustic, hydrodynamic, optic, and particle. Out of these four techniques only acoustic and hydrodynamic cavitation are most widely used, as they are efficient in bringing about the desired chemical changes.

Acoustic Cavitation. The cavities are produced by passing the sound waves, usually ultrasound (>16 kHz), through the liquid medium.

Hydrodynamic Cavitation. The cavitation is produced by pressure variation in a flowing liquid which is obtained by providing flow constrictions such as orifice and venturi. When the liquid passes through the constriction, the kinetic energy/velocity increases at the expense of the pressure. When the pressure at the throat or vena contracta falls below the vapor pressure of the liquid, the liquid flashes generating a number of vaporous cavities. These cavities are then collapsed when they came in downstream of constriction where the pressure recovers.

The aim of this work is to study the degradation of Acid Red 88 dye (AR88) using hydrodynamic cavitation and to investigate the effect of additives (H_2O_2 and catalyst) on the overall degradation

Special Issue: Nigam Issue

Received: February 3, 2011
Accepted: March 15, 2011
Revised: March 7, 2011
Published: April 01, 2011

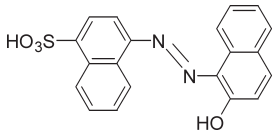

Figure 1. Molecular structure of Acid Red 88.

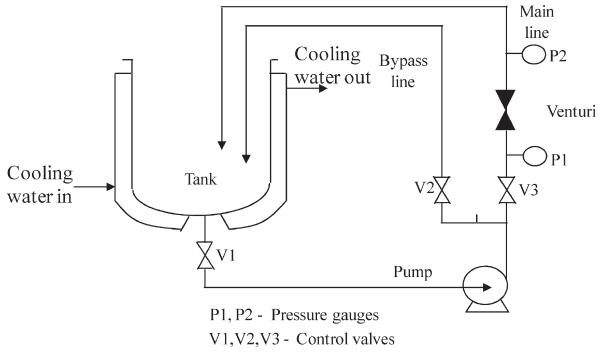

Figure 2. Schematic representation of hydrodynamic cavitation reactor setup.

rate. Additionally, a comparative study of hydrodynamic cavitation and acoustic cavitation has also been carried out.

2. MATERIAL AND METHODS

2.1. Materials. Acid Red 88 dye (molecular weight, 400.38 g/mol; IUPAC name, 4-(2-Hydroxy-1-naphthylazo)-1-naphthalenesulfonic acid sodium salt; molecular formula: $C_{20}H_{13}N_2O_4S.Na$) was procured from ATUL Limited, India, as a gift sample and hydrogen peroxide was purchased from SD fine chemicals (India). The chemical structure of acid red 88 dye is shown in Figure 1.Titanium dioxide (TiO_2, Degussa P25, Germany) with a specific surface area of 57 $m^2\ g^{-1}$ was used as a starting material to prepare Fe−TiO_2 nanocatalyst. The experiments were carried out within the temperature range of 35−40 °C. All the solutions were prepared with distilled water as a dissolution medium.

2.2. Preparation of Fe−TiO_2 nanocatalyst. Nanosized Fe−TiO_2 was prepared by the impregnation method as reported in the literature.[17] Calculated amount of previously calcined TiO_2 (at 400 °C for 5 h) was mixed with an aqueous solution of $FeNO_3 \cdot 9H_2O$ (2 atomic wt %). The mixture was stirred for 48 h to allow the penetration of iron ions into the titanium dioxide crystal matrix and then the supernatant was evaporated by heating the mixture at 100 °C over a period of 24 h. The resultant product was calcined at 550 °C for 5 h.

2.3. Hydrodynamic Cavitation Reactor. The experimental setup is shown in Figure 2. The setup includes a holding tank of 15 L volume, a positive displacement pump of power rating 1.1 kW, control valves (V1, V2, and V3), flanges to accommodate the cavitating device, a main line, and a bypass line. The suction side of the pump is connected to the bottom of the tank, and discharge from the pump branches into two lines: the main line and a bypass line. The main line consists of a flange which houses the cavitating device which can be either orifice or venturi. The bypass line is provided to control the liquid flow through the main line. Both the mainline and bypass line terminate well inside the tank below the liquid level to avoid any induction of air into the liquid. Figure 3 shows the cavitating device (venturi) used in this work.

2.4. Degradation of Acid Red 88 dye. Surface morphology, particle size, and the various contours of the catalyst powders were analyzed by XRD (Philips PW1710 diffractometer, Cukα radiation, Holland) and transmission electron microscopy (recorded using TECNAI G^2 model), respectively. The surface area of the samples was measured with the assistance of Flowsorb II 2300 of Micrometrics, Inc.

Hydrodynamic-cavitation-based degradation of AR88 was carried out at different conditions using a fixed solution volume of 4 L and for a constant circulation time of 2 h. The temperature of the solution during experiments was kept constant in all the cases at about 35 °C and maintained by circulating cooling water through the jacket provided. The degradation of dye was analyzed by two means: one by observing the decolorization and the second by analyzing the complete mineralization of dye. The decolorization is due to the breakage of chromophore group (N═N), whereas mineralization is the complete oxidation of the dye molecule into CO_2 and H_2O. The decolorization of AR88 was analyzed by measuring the absorbance of dye solution at 506 nm after treating it for a fixed interval of time, using a UV-spectrophotometer (Shimadzu-1800), and the mineralization was analyzed by measuring the total organic carbon (TOC) content of the dye solution using a TOC analyzer (ANATOC II, SGE International Pty Ltd., Australia). The optimization of initial concentration, inlet pressure, solution pH, and catalyst loading was done by measuring the rate constant of the decolorization process, and then subsequently the TOC was measured at different optimized parameters. The optimization of H_2O_2 concentration was done by analyzing the rate of mineralization process as well as by decolorization. Acoustic-cavitation-based degradation of AR88 was carried out using an ultrasonic horn having a longitudinal horn (capacity of 7 lit, surface area = 290 cm^2, driving frequency of 25 kHz, power input of 1 kW, power density = 0.14 W/cm^3).

3. RESULT AND DISCUSSION

3.1. Characterization of Fe−TiO_2 Nanocatalyst. To investigate the changes in the crystal structure due to Fe doping, X-ray diffraction measurements were taken in the range of 2θ = 20−80° for the Fe−TiO_2 and bare TiO_2 photocatalysts. The detected major peaks for the modified and unmodified samples appeared to be the same, but the intensities of the peaks were found to be significantly reduced in the case of Fe−TiO_2. In addition, peak broadening was noticed, which might be related to grain refinement due to doping. It is believed that Fe^{3+} with ionic radius (0.69 Å) is very close to semiconductor lattice (Ti^{4+} radius is 0.745 Å) and may penetrate into the semiconductor lattice,[18] and thus the iron ions were distributed uniformly in the interstices of the semiconductor crystalline structure.[19] Hence, there is a possibility for formation of $FeTiO_3$ by the intervalence charge transfer between Fe^{3+} and Ti^{4+} which is identified by a diffraction peak at the 2θ value 48.93° (JCPDS 75-1211).[20−22] Further on viewing the XRD spectra, bare TiO_2 and Fe−TiO_2 samples showing a peak at the 2θ value 25.3° (JCPDS 21-1272) confirms that the anatase structure is predominantly present in the crystal structure (Figure 4). Scherrer formula was used to calculate the particle size of the prepared photocatalyst and it was found to be ∼30 nm. Lastly, no Fe_2O_3 phase formation was detected in the present study, this may be due to the low loading of iron (2 atomic weight %).[23]

To obtain further insight into the nature of the metal dopant, a detailed TEM analysis was carried out for the prepared Fe−TiO_2

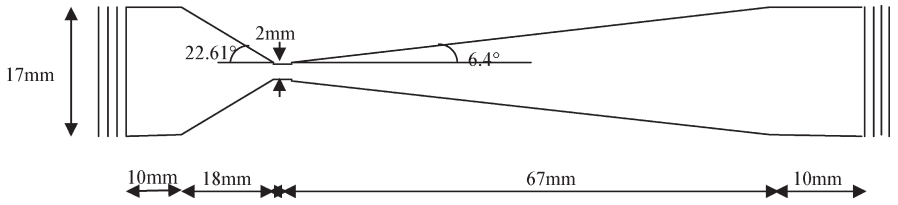

Figure 3. Schematic of venturi.

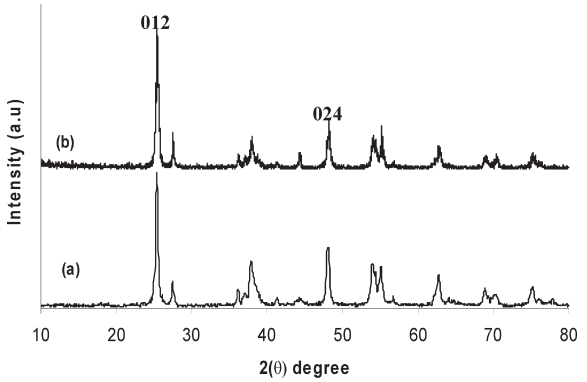

Figure 4. X -ray diffraction pattern of (a) TiO_2 and (b) Fe−TiO_2.

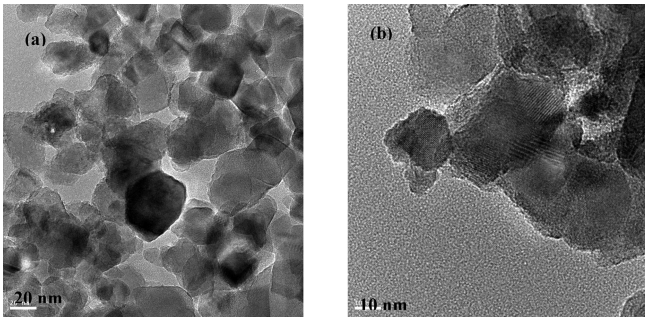

Figure 5. (a) Representative TEM image of Fe−TiO_2 nanoparticles and (b) the corresponding high resolution TEM images.

nanocatalyst which showed direct information about the distribution of the dopant on the semiconductor surface (Figure 5). The bright gray particles in the micrographs are obviously titania and the iron dopants have been observed as the dark patches on the gray surface of titania. The TEM image reveals that the crystallinity of the photocatalysts has been increased which is indicated by the increased crystal size with well developed faces of Fe−TiO_2 (Figure 5a). Further, upon clear examination at higher magnification, the crystal lattice fringes are clearly visible for Fe−TiO_2 (Figure 5b). Moreover TiO_2 can act as support to adsorb Fe^{3+} ion precursors and hence the particle size of iron-doped TiO_2 formed is found to be ~30 nm. The TEM micrograph results are consistent with the crystal size calculated by the Scherrer equation from the XRD pattern. The BET surface area of 38 $m^2\ g^{-1}$ for the Fe−TiO_2 sample was significantly lower compared to that of the bare TiO_2 (57 $m^2\ g^{-1}$). The observed decrease in the specific surface area of the catalyst suggests that the incorporation of iron has blocked some of the pores by the penetration of the same.

3.2. Hydraulic Characteristics. To investigate the hydraulic characteristics of venturi used in this study, the main line flow rate and cavitation number at different inlet pressure were measured and then calculated. Table 1 shows the value of cavitation number, mainline flow rate and the velocity at the throat of venturi. Appendix A shows one typical set of calculation, carried out to complete Table 1.

The cavitation number is a dimensionless number used to characterize the condition of cavitation in a hydraulic device. The cavitation number is defined as

$$C_v = \left(\frac{p_2 - p_v}{\frac{1}{2}\rho v_o^2} \right) \quad (1)$$

where, p_2 is the fully recovered downstream pressure, p_v is the vapor pressure of the liquid, v_o is the velocity at the throat of the cavitating constriction which can be calculated by knowing the main line flow rate and diameter of venturi. Under ideal condition cavities are grown when $C_v \leq 1$, but in some cases cavities can grow at a value of C_v greater than 1 due to the presence of some dissolved gases and suspended particles which provide additional nuclei for the cavities to form. It was found that the cavitation number decreases with an increase in inlet pressure to the venturi. As an increase in inlet pressure increases the main line flow rate, the velocity (v_o) at the throat also increases, which subsequently reduces the cavitation number. Senthilkumar and Pandit[3] have shown that cavitation number decreases with an increase in the inlet pressure resulting in lower cavitational intensity (collapse pressure), but at the same time the number of cavities generated and collapsing per unit time increases.

3.3. Effect of Initial Dye Concentration. To investigate the effect of initial concentration of dye on degradation rate and to find out the kinetics of degradation, experiments were conducted with different initial concentration ranging from 50 to 150 μM. The operating pressure and the pH of solution were kept constant in all the experiments at 5 bar and 2.0, respectively. Rates were calculated at different initial dye concentration. In the case of degradation of the dye where the concentration of dye is very small (<150 μM) the rate can be expressed as follows:

$$R_A = kC_A^n \quad (2)$$

$$\ln(R_A) = \ln(k) + n \ln(C_A) \quad (3)$$

Where, R_A is the rate of degradation of dye in mol L^{-1} min^{-1}, C_A is the concentration of dye in mol/L, k is the rate constant (L^{n-1} mol^{n-1} min^{-1}) and n is the order of reaction.

Figure 6 shows the plot of $\ln(R_A)$ vs $\ln(C_A)$, the slope of which gives the order of reaction. From Figure 6 it is clear that the degradation of AR88 follows first order kinetics and also the plot of rate vs concentration (Figure 7) is a straight line passing through the origin, which also conforms that the degradation of AR88 is a first order reaction. The rate of degradation increases with an increase in initial concentration of dye, and the first order

Table 1. Flow Characteristics of Venturi

sr. no.	inlet pressure (bar)	flow rate (LPH)	velocity (m/s)	cavitation number (C_v)
1	0.2	96	8.49	2.69
2	0.5	200	17.68	0.62
3	1	235	20.78	0.45
4	1.5	260	22.99	0.37
5	2	288	25.46	0.3
6	3	340	30.06	0.21
7	4	375	33.16	0.18
8[a]	5	410	36.30	0.15
9	6	445	39.35	0.13
10	7	470	41.56	0.11
11	10	525	46.42	0.09

[a] Sample calculation Appendix A.

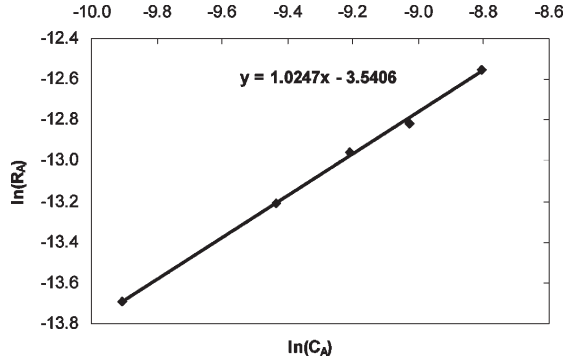

Figure 6. First order degradation of AR88. Conditions: volume of solution, 4 L; inlet pressure, 5 bar; pH of solution, 2.0.

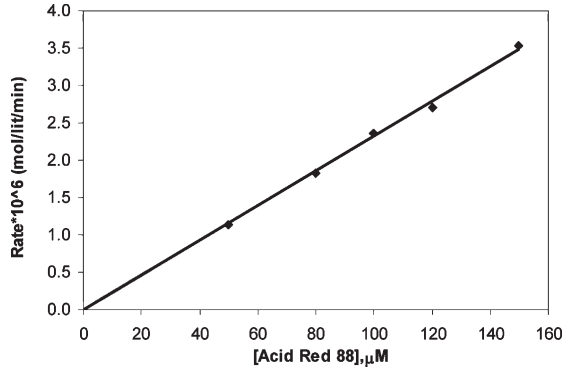

Figure 7. Effect of initial concentration on degradation rate. Conditions: volume of solution, 4 L; inlet pressure, 5 bar; pH of solution, 2.0.

rate constant calculated was found to be constant, irrespective of initial dye concentration, confirming the validity of the kinetic expression.

3.4. Effect of Inlet Pressure. The most important parameter in the case of hydrodynamic-cavitation-based degradation of pollutant is the inlet fluid pressure to the cavitating device. As mentioned earlier, the inlet fluid pressure and the velocity at the throat are dependent on each other, and it affects the cavitating condition inside the venturi, so optimization of inlet pressure is

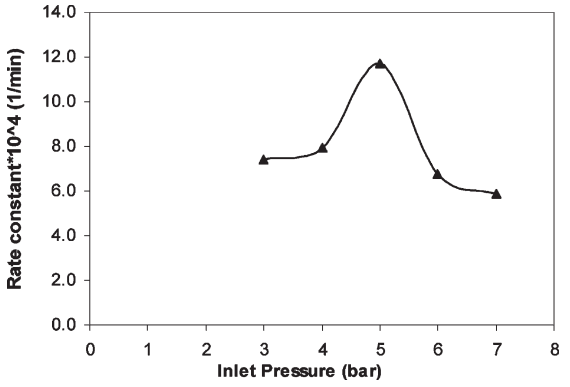

Figure 8. Effect of inlet pressure on decolorization rate of AR88. Conditions: volume of solution, 4 L; initial concentration, 100 μM; pH of solution, 5.8.

necessary in order to get maximum cavitational effects. To investigate the effect of inlet pressure on the degradation rate, the experiments were carried out at different inlet pressure varying from 3 to 7 bar. The concentration of AR88 and the pH of the solution were kept constant in all the experiments at 100 μM and 5.8, respectively. Figure 8 shows the effect of inlet pressure on the decolorization rate of AR88. It was found that decolorization rate increases with an increase in inlet pressure reaching to the maximum at 5 bar inlet pressure and then decreases. As the pressure increases, the main line flow rate housing the cavitating device increases, so the number of passes of the liquid through the venturi increases. This increase in the number of passes causes the liquid to go through the cavitating device (venturi in this case) several times and to experience the cavitating condition for a longer time, due to which cavitational yield increases. Senthilkumar and Pandit[3] have shown that cavitation number decreases with an increase in the inlet pressure due to increased liquid flow and velocity. A decrease in cavitation number results into lower cavitational intensity (collapse pressure), but at the same time the number of cavities generated and collapsing event per unit time, per unit volume increases. Gogate and Pandit[24] have concluded that there is an optimum pressure at which cavitational intensity is maximum and have explained that the quantum of the total collapse pressure is the result of collapse pressure due to a single cavity and number of cavities being generated. Tullis[25] have also observed that as the cavitation number decreases, more number of cavities are formed and once the cavitation device is filled with a lot of cavities these cavities start coalescing to form a larger bubble. These larger bubbles escape the liquid without collapsing, thus reducing the cavitational yield (reduced decolorization rate after 5 bar of operating fluid pressure).

3.5. Effect of pH. The pH of the solution is another important parameter in deciding the rates of degradation and hence the overall efficiency. The effect of pH was investigated by carrying out experiments at different pH in the range 2−11. Figure 9 shows the effect of pH on the decolorization rate of AR88. The results indicate that the rate of decolorization increases with a decrease in solution pH, that is, acidic medium is more favorable for the degradation of dye. A much lower decolorization rate was observed at pH 10.0. About 92% decolorization and 35% reduction in TOC was obtained at pH 2.0 using HC. The enhancement in the decolorization/degradation rate at lower pH can be attributed to the fact that dye molecule is present in

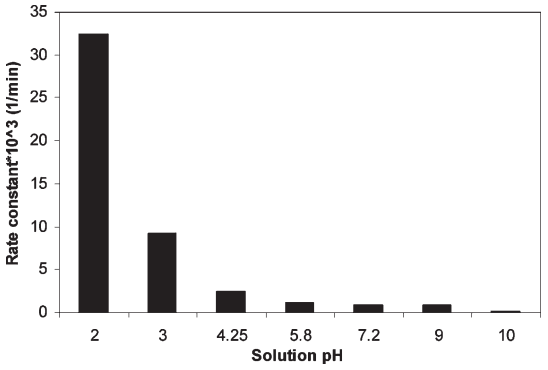

Figure 9. Effect of solution pH on decolorization rate of AR88 Conditions: volume of solution, 4 L; initial concentration, 100 μM; inlet pressure, 5 bar.

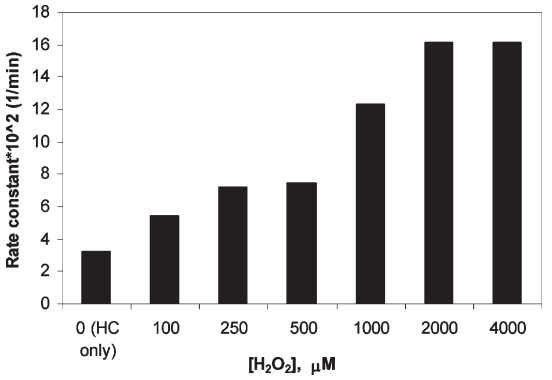

Figure 10. Effect of H_2O_2 addition on decolorization rate of AR88. Conditions: volume of solution, 4 L; initial concentration, 100 μM; pH of solution, 2.0; inlet pressure, 5 bar.

the molecular state at lower pH when the pH is less than the pK_a value (10.7) of AR88, and hence can easily enter the gas−water interface of cavities due to hydrophobic nature and thus, is more readily subjected to the OH radical attack and also to the thermal decomposition, whereas in the basic medium the dye molecules gets ionized and become hydrophilic in nature thereby remaining in the bulk liquid. As only about 10% of the OH radicals generated in the cavity can diffuse into the bulk solution,[26] the concentration of OH radicals in the bulk solution reduces and hence the decolorization rate decreases. Lin and Ma[27] have studied the effect of pH on the degradation of 2-chlorophenol using ultrasound and showed that the rate constant of 2-chlorophenol decomposition at pH 3 was almost 40 times greater than at pH 11. They have calculated the extent of ionization at different pH, and found that when the pH value is greater than the pK_a (8.49) value of 2-chlorophenol, almost all of the 2-chlorophenol is ionized in the solution, and when the pH value is less than the pK_a value, almost all of the 2-chlorophenol is in the molecular form.

Ince and Guyer[28] have studied the effect and hence the subsequent impacts of pH and molecular structure on ultrasonic degradation of azo dyes. They have explained that the acceleration in decolorization of dye by acidification is due to neutralization of the dyes upon protonation of negatively charged SO_3^- sites, and the hydrophobic enrichment of the molecules to enhance their reactivity under ultrasonic cavitation. While percentage reduction in decolorization under alkaline conditions is a consequence of ionization of the dyes by hydrogen loss from protonated sites and naphthol−OH, resulting in enhanced hydrophilic character to the dye, which does not accumulate at the cavity-water interface and hence is affected lower by the cavitational event.

Thus, the effect of hydrodynamic cavitation on degradation will be very much dependent on the utilization of free radicals by the pollutant molecules. Operating pH, state of molecule (whether molecular or ionic), and nature (hydrophobic and hydrophilic) are the important parameters which ultimately decide the efficient degradation of pollutants. The transient nature of the OH radicals and the vicinity of the pollutant molecule are the two main parameters deciding the final observed degradation rate.

3.6. Effect of H_2O_2. The main driving mechanism in the case of hydrodynamic cavitation-based-degradation of dye is the formation and subsequent attack of hydroxyl radicals and thermal decomposition. In the case of reaction, where the controlling mechanism is the free radical attack, use of hydrogen peroxide should enhance the degradation rate. The effect of the addition of H_2O_2 on the degradation rate was studied by varying the concentration of H_2O_2 ranging from 100 to 6000 μM and keeping pressure and dye concentration constant at 5 bar and 100 μM, respectively. Figure 10 shows the effect of H_2O_2 on the decolorization rate of AR88. Table 2 shows the value of rate constant for the decolorization and mineralization of AR88 and also the percentage reduction in color and TOC. It was found that the rate of decolorization increases with an increase in concentration of H_2O_2 from 0 to 4000 μM and almost 100% decolorization takes place at 4000 μM. The rate constant for the decolorization remains constant with further increase in the concentration of H_2O_2, that is, beyond 4000 μM. But the analysis of TOC shows that there is an optimum concentration of H_2O_2 at which the mineralization of dye is maximum. The rate constant for the reduction in TOC increases with an increase in concentration of H_2O_2 up to 4000 μM and decreases thereafter. Thus, the optimum concentration of hydrogen peroxide can be considered as 4000 μM, which gives a molar ratio of 40:1 (H_2O_2/dye concentration). Around 72% reduction in TOC and almost 100% reduction in color were obtained in case of HC with the addition of 4000 μM H_2O_2. It was also observed that only 4.6% decolorization takes place in normal stirring (no HC) with the addition of 4000 μM H_2O_2; that is, the combination of hydrodynamic cavitation and H_2O_2 gives a better result as compared to individual operation of these advanced oxidation processes. The addition of H_2O_2 provides the additional hydroxyl radicals for the oxidation of dye but it also acts as a scavenger of the generated free radicals and therefore the combined effect of HC and H_2O_2 will be very much dependent on the utilization of the generated free radicals by the dye molecules. Teo et al.[29] have also reported a similar conclusion about the effect of H_2O_2 on the degradation of *p*-chlorophenol using ultrasound. They have reported that the degradation rate increases with an increase in the hydrogen peroxide concentration reaching to the maximum at 20 mM concentration of H_2O_2 for an initial concentration of 0.4 mM (giving an optimum molar ratio of 50:1) which is very similar to the optimum found in this work. Chen et al.[30] have studied the synergetic effect of hydrogen peroxide and ultrasound on the degradation of chloroform. The molar ratio of hydrogen peroxide to chloroform concentration was varied in the range 12−120 and an optimum concentration of hydrogen peroxide was again reported to be 30 times the concentration of chloroform.

Table 2. Effect of H_2O_2 Addition on Degradation of AR88[a]

System	rate constant $\times 10^2$ min^{-1} for decolorization process	rate constant $\times 10^2$ min^{-1} for mineralization process	% decolorization	% reduction in TOC
HC only	3.24	1.18	92.00	35.70
HC + 500 μM H_2O_2	7.46	1.35	92.80	42.80
HC + 1000 μM H_2O_2	12.30	1.91	94.30	57.14
HC + 2000 μM H_2O_2	16.10	2.62	98.40	64.30
HC + 4000 μM H_2O_2	16.10	3.02	99.00	71.42
HC + 6000 μM H_2O_2	16.10	1.89	98.40	57.14

[a] Conditions: volume of solution, 4 L; initial concentration, 100 μM; pH of solution, 2.0; inlet pressure, 5 bar.

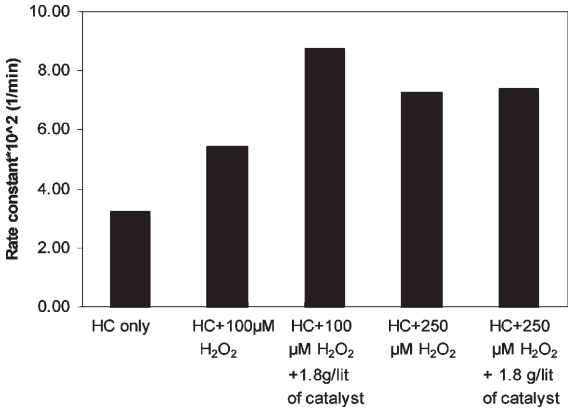

Figure 11. Effect of catalyst addition on decolorization rate of AR88. Conditions: volume of solution, 4 L; initial concentration, 100 μM; pH of solution, 2.0; inlet pressure, 5 bar.

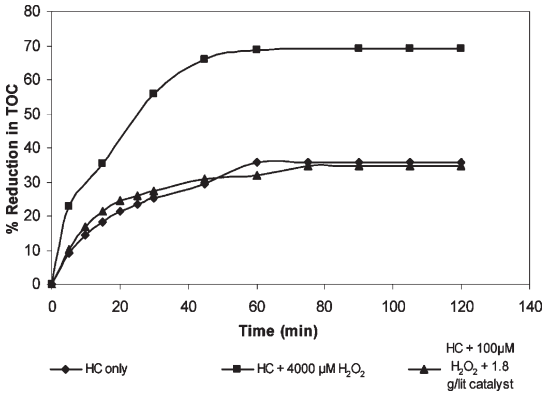

Figure 12. Reduction (%) in TOC as a function of time at different optimized conditions: volume of solution, 4 L; initial concentration, 100 μM; pH of solution, 2.0; inlet pressure, 5 bar.

3.7. Effect of Catalyst. The presence of additives in the system enhances the process of cavity generation and hence intensifies the cavitational activity in the reactor. The additives can be in the form of solid particles or the additives can have catalytic action in terms of promoting the rates of dissociation of the oxidants such as ozone or hydrogen peroxide, scavenging the undesired radical species. Figure 11 shows the effect of catalyst loading on the decolorization of AR88. It was found that the rate of decolorization of dye was enhanced (by about 45−60%) by the addition of catalyst (Fe−TiO_2; 1.8 g/L) over the use of only H_2O_2, when the molar ratio of hydrogen peroxide to dye concentration was kept at 1:1. The rate constant was found to be 8.75×10^{-2} min^{-1} in the case of hydrodynamic cavitation with the addition of catalyst and in the presence of H_2O_2 as compared to 5.42×10^{-2} min^{-1} in the absence of catalyst at equivalent H_2O_2 loading. While at the molar ratio of 2 (H_2O_2: dye concentration) and catalyst loading of 1.8 g/L there was no enhancement in the decolorization rate of the dye. The percentage reduction in TOC and the rate constant for the TOC reduction was the same in all the cases. About 35% reduction in TOC was observed in all the cases. So, it was concluded that the addition of catalyst improves the decolorization process to some extent, but it is not able to enhance the complete mineralization process. The presence of solid particles provides the additional nuclei for the formation of cavities and hence the number of cavitational events occurring in the reactor is enhanced resulting in an increased cavitational activity, thereby increasing the decolorization rate. Since this catalyst is also coated with Fe ion (Fe^{3+}), it initiates the Fenton-like chemistry and hence an increase in the extent of hydroxyl radical generation resulting in an increased decolorization rate. Pandit et al.[31] studied the ultrasonic degradation of 2:4:6 trichlorophenol in the presence of TiO_2 catalyst and found that degradation of 2,4,6-trichlorophenol is higher under the influence of the ultrasound in the presence of the catalyst TiO_2 compared to that when catalyst was absent. Nagata et al.[16] studied the effect of Fe (II) ions on the degradation of 3-chlorophenol using sonolysis and suggested that there is an optimum concentration of Fe (II) for the degradation of 3-chlorophenol and an excessive amount of Fe (II) leads to a decrease in the degradation rate because of the scavenging of the hydroxyl radicals due to the presence of oxidizable form of Fe (Fe^{2+} instead of Fe^{3+}). The degradation of 3-CP was enhanced in the presence of Fe(II): the rate increased to 2.4 times at 1 mM of Fe(II) concentration and to only 1.5 times at 2 mM.

3.8. Mineralization Studies. In the study of the effect of various parameters on degradation rate, the concentration of dye was measured at different time intervals and then rate constants were calculated, but the reduction in dye concentration does not mean that dye is degraded completely. As in the case of hydrodynamic cavitation the degradation of dye is done by the attack of hydroxyl radicals on the dye molecules resulting in oxidation of dye molecules into some intermediate. These intermediates further react with other hydroxyl radicals to give final products like CO_2, H_2O, etc. These intermediates are expected to be aromatic compounds which also accounts for the TOC of solution. Therefore, to get the complete picture about the degradation of AR88, the TOC was measured at different optimized parameters. Figure 12 shows the percentage reduction in TOC with respect to time at optimized conditions under different types of experimental conditions such as only using HC, HC + H_2O_2, or HC + H_2O_2 + catalyst. It was found that mineralization of dye is a relatively slow process as

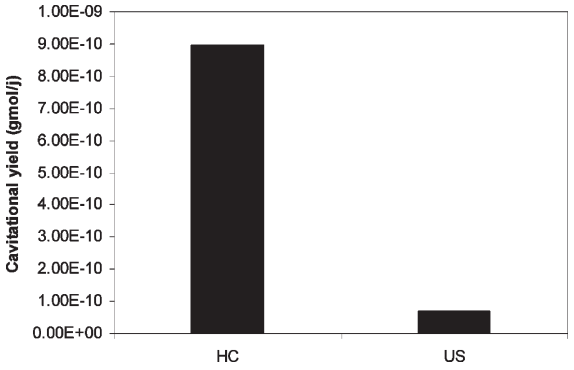

Figure 13. Cavitational yield for hydrodynamic cavitation and acoustic cavitation (US: ultrasound/acoustic cavitation).

compared to decolorization which is only due to the breakage of chromophore. This may also be due to the side reactions of hydroxyl radicals taking place in the solution, resulting in a lower amount of OH radicals being made available for the further oxidation of intermediates. It was found that TOC reduced by 35% of the original, while 92% decolorization was observed when the degradation was carried out in hydrodynamic cavitation alone, and it increases to 72% (100% decolorization) with the addition of 4000 μM of H_2O_2, while there was no further enhancement in the TOC reduction with the addition of catalyst.

3.9. Comparison between Hydrodynamic Cavitation and Acoustic Cavitation. To date most of the research work has been done on acoustic-cavitation-based degradation of various pollutants. Though, highly successful in laboratory scale operation, acoustic cavitation still has not been able to find its application at industrial scale operation due to problems associated with construction of high frequency transducers and also the cost of materials and energy requirements. The advantages of a hydrodynamic cavitational reactor is that it is easy to operate and design and also the cost of material is small. The system can be run in a continuous cycle, and also a large volume of solution can be handled. Some literature[32−35] shows that hydrodynamic cavitation is more energy efficient than acoustic cavitation. Here, the comparison between hydrodynamic cavitation and acoustic cavitation has been done on the basis of cavitational yield. The cavitational yield is defined as the ratio of the cavitational effect (moles of dye degraded) to the total energy input to the system. The experiments were carried out at fixed initial concentration of AR88 (100 μM) and at pH 2 for a fixed time of operation (2 h) for both types of reactor. The longitudinal horn-type acoustic cavitational reactor having 25 kHz frequency and 1 kW power was used. Experiments in the hydrodynamic cavitational reactor were carried out at an optimum operating fluid pressure of 5 bar. Figure 13 shows the cavitational yield of both processes at pH 2. It was found that the cavitational yield in the case of hydrodynamic cavitation is 13 times higher than acoustic cavitation (detailed calculation is given in appendix B). The rate constant was found to be 32.4×10^{-3} min^{-1} in the case of hydrodynamic cavitation as compared to 1.36×10^{-3} min^{-1} in the case of acoustic cavitation. Senthilkumar et al.[33] have shown that the cavitational yield for hydrodynamic cavitation is 3 times higher than that for acoustic cavitation. The basic reason for the low cavitational yield of ultrasonic equipment is due to poor energy conversion efficiency. Gogate and Pandit[34] have shown the energy efficiency and cavitational yield for different reactors for the model reaction of decomposition of KI and have shown that the cavitational yield as well as the energy efficiency is much higher for the hydrodynamic cavitation reactor. Sivakumar and Pandit[35] have also shown that cavitational yield for the hydrodynamic cavitation is higher as compared to that of any of the ultrasonic equipment studied for the degradation of rhodamine B, water-soluble dye. They have shown that the cavitational yield for the hydrodynamic cavitation is 12 times higher than that for ultrasonic equipment having 25 kHz frequency. Hung and Hoffman[36] carried out the degradation of chlorinated hydrocarbons and have compared different ultrasonic equipment with frequencies in the range of 20−1078 kHz. They have shown that the degradation of CCl_4 is 3 times higher at 500 kHz as compared to that at 20 kHz frequency. Petrier et.al.[37] have also shown that the degradation of phenol is approximately six times higher at 487 kHz than at 20 kHz. So even if we compare HC with ultrasonic equipments having higher frequency as mentioned in the literature we can still conclude that the cavitational yield for HC is significantly higher as compared to that for acoustic cavitation. The cavitational yield for HC is much higher (13 times) as against 3 times and 6 times higher obtained in higher frequency (≈500 kHz) ultrasonic equipments as compared to that in lower frequency (25 kHz) ultrasonic equipment.

4. CONCLUSIONS

The conclusions drawn from this study can be summarized as follows: (1) The present work has shown that Acid Red 88 dye can be effectively degraded by hydrodynamic cavitation and this degradation followed first order reaction kinetics. Hydrodynamic cavitation is favored under acidic condition and is very much dependent on the solution pH, state (whether molecular or ionic), and nature (hydrophobic or hydrophilic) of the pollutants. (2) The addition of H_2O_2 enhances the degradation rate due to additional hydroxyl radicals available for the oxidation of dye. The degradation of dye increases with an increase in the concentration of H_2O_2 up to an optimum value and decreases afterward due to scavenging of hydroxyl radicals by H_2O_2 itself. The addition of catalyst also enhances the decolorization rate to some extent but fails to enhance the mineralization of dye. (3) The hydrodynamic cavitation is more energy efficient as compared to acoustic cavitation and an almost 13 times higher cavitational yield was obtained in case of hydrodynamic cavitation as compared to that in acoustic cavitation.

■ APPENDIX A: SAMPLE CALCULATION FOR THE ESTIMATION OF HYDRAULIC CHARACTERISTICS—TABLE 1

Calculation for Sr. No. 8, Table 1

Inlet fluid pressure = 601325 Pa
Downstream pressure (p_2) = 101325 Pa
Vapor pressure of water at 30 °C (p_v) = 4242.14 Pa
Volumetric flow rate (V) = 410 LPH = 1.14×10^{-4} m^3/s
Diameter of the throat of the venturi (d_o) = 2 mm
Flow area:

$$(a_o) = \frac{\pi}{4} d_o{}^2 = \frac{\pi}{4} \times (2 \times 10^{-3})^2 = 3.14 \times 10^{-6}\ m^2$$

Velocity at the throat of the venturi:

$$(v_o) = \left(\frac{V}{a_o}\right) = \left(\frac{1.14 \times 10^{-4}}{3.14 \times 10^{-6}}\right) = 36.30\ m/s$$

Cavitation number:

$$(C_v) = \frac{(p_2 - p_v)}{\left(\frac{1}{2}\rho {v_o}^2\right)} = \frac{(101325 - 4242.14)}{\left(\frac{1}{2} \times 1000 \times 36.30^2\right)} = 0.15$$

APPENDIX B: SAMPLE CALCULATION FOR THE ESTIMATION OF CAVITATIONAL YIELD: FIGURE 13

Cavitational Yield for Acoustic Cavitation

Calorimetric efficiency of horn = 20.0%

The power dissipated into the solution in 2 h

$$= \text{power} \times \text{efficiency} \times \text{time} = 1000 \times 0.2 \times (2 \times 3600) = 1440000 \text{ J}$$

Number of moles of dye degraded

$$= 14.04 \times 10^{-6} \text{ (gmol/L)} \times 7 \text{ (L)} = 9.83 \times 10^{-5} \text{ gmol}$$

Cavitational yield

$$= \left(\frac{9.83 \times 10^{-5}}{1440000}\right) = 6.82 \times 10^{-11} \text{ gmol/J}$$

Cavitational Yield for Hydrodynamic Cavitation

Pressure drop across the venturi (ΔP) = 5 bar

Volumetric flow rate (Q) at pressure 5 bar = 1.14×10^{-4} m^3/s

Power dissipated into the solution in 2 h

$$= \Delta P \times Q \times \text{time} = 500000 \times (1.14 \times 10^{-4}) \times (2 \times 3600) = 410400 \text{ J}$$

Number of moles of dye degraded

$$= 92 \times 10^{-6} \text{ (gmol/l)} \times 4 \text{ (L)} = 36.8 \times 10^{-5} \text{gmol}$$

$$\text{cavitational yield} = \left(\frac{36.8 \times 10^{-5}}{410400}\right) = 8.97 \times 10^{-10} \text{ gmol/J}$$

AUTHOR INFORMATION

Corresponding Author

*E-mail: ab.pandit@ictmumbai.edu.in. Tel.: +91-22-3361 2012. Fax: +91-22-4145614.

ACKNOWLEDGMENT

V. K. Saharan would like to thank DIISR, Australia, and DST, GOI, for providing financial support under the India−Australia Strategic Research Funding Program.

REFERENCES

(1) Adewuyi, Y. G. Sonochemistry: Environmental science and engineering applications. *Ind. Eng. Chem. Res.* **2001**, *40*, 4681.

(2) Lorimer, J. P.; Manson, T. J. Sonochemistry: Part 1−The physical aspects. *Chem. Soc. Rev.* **1987**, *16*, 239.

(3) Senthilkumar, P.; Pandit, A. B. Modeling hydrodynamic cavitation. *Chem. Eng. Technol.* **1999**, *22*, 1017.

(4) Anandan, S.; Ashokkumar, M. Sonochemical synthesis of Au−TiO_2 nanoparticles for the sonophotocatalytic degradation of organic pollutants in aqueous environment. *Ultrason. Sonochem.* **2009**, *16*, 316.

(5) Bhatkhande, D. S.; Pangarkar, V. G.; Beenackers, A. A. C. M. Photocatalytic degradation for environmental applications: A review. *J. Chem. Technol. Biotechnol.* **2002**, *77*, 102.

(6) Legrini, O.; Oliveros, E.; Braun, A. M. Photochemical processes for water treatment. *Chem. Rev.* **1993**, *93*, 671.

(7) SathishKumar, P.; Ruby Raj, M.; Anandan, S.; Zhou, M.; Ashokkumar, M. Visible light-assisted photocatalytic degradation of acid red 88 using Au−ZnO nanophotocatalysts. *Water Sci. Technol.* **2009**, *60*, 1589.

(8) Bigda, R. J. Fenton's chemistry: An effective advanced oxidation process. *Environ. Technol.* **1996**, *6*, 34.

(9) Echigo, S.; Yamada, H.; Matsui, S.; Kawanishi, S.; Shishida, K. Comparison between O_3/VUV, O_3/H_2O_2, VUV and O_3 processes for the decomposition of organophosphoric acid trimesters. *Water Sci. Technol.* **1996**, *34*, 81.

(10) Weavers, L. K.; Hoffmann, M. R. Sonolytic decomposition of ozone in aqueous solution: Mass transfer effects. *Environ. Sci. Technol.* **1998**, *32*, 3941.

(11) Anandan, S.; Lee, G.; Chen, P.; Fan, C.; Wu, J. J. Removal of orange II dye in water by visible light-assisted photocatalytic ozonation using Bi_2O_3 and Au/Bi_2O_3 nanorods. *Ind. Eng. Chem. Res.* **2010**, *49*, 9729.

(12) Pinjari, D. V.; Pandit, A. B. Cavitation milling of natural cellulose to nanofibrils. *Ultrason. Sonochem.* **2010**, *17*, 845.

(13) Weavers, L. K.; Ling, F. H.; Hoffmann, M. R. Aromatic compound degradation in water using a combination of sonolysis and ozonolysis. *Environ. Sci. Technol.* **1998**, *32*, 2727.

(14) Kang, J. W.; Hoffmann, M. R. Kinetic and mechanism of the sonolytic destruction of methyl *tert*-butyl ether by ultrasonic irradiation in the presence of ozone. *Environ. Sci. Technol.* **1998**, *32*, 3194.

(15) Hoffmann, M. R.; Hua, I.; Hochemer, R. Application of ultrasonic irradiation for the degradation of chemical contaminants in water. *Ultrason. Sonochem.* **1996**, *3*, 163.

(16) Nagata, Y.; Nakagawa, M.; Okuno, H.; Mizukoshi, Y.; Yim, B.; Maeda, Y. Sonochemical degradation of chlorophenols in water. *Ultrason. Sonochem.* **2000**, *7*, 115.

(17) Bickley, R. I.; Lees, J. S.; Tilley, R. J. D.; Palmisano, L.; Schiavello, M. Characterization of iron/titanium oxide photocatalysts. Part 1. Structural and magnetic studies. *J. Chem. Soc. Faraday Trans.* **1992**, *88*, 377.

(18) Ahrens, L. H. The use of ionization potentials Part 1. Ionic radii of the elements. *Geochim. Cosmochim. Acta* **1952**, *2*, 155.

(19) Wang, J A.; Limas-Ballesteros, R.; Lopez, T.; Moreno, A.; Gomez, R.; Novaro, O.; Bokhimi, X. Quantitative determination of titanium lattice defects and solid-state reaction mechanism in iron-doped TiO_2 photocatalysts. *J. Phys. Chem. B* **2001**, *105*, 9692.

(20) Ishikawa, Y.; Akimoto, S. Magnetic property and crystal chemistry of ilmenite ($MeTiO_3$) and hematite (αFe_2O_3) system I. crystal chemistry. *J. Phys. Soc. Jpn.* **1958**, *13*, 1110.

(21) McDonald, P. F.; Parasiris, A.; Pandey, R. K.; Gries, B. L.; Kirk, W. P. Paramagnetic resonance and susceptibility of ilmenite, $FeTiO_3$ crystal. *J. App. Phys.* **1991**, *69*, 1104.

(22) Kim, Y. J.; Gao, B.; Han, S. Y.; Jung, M. H.; Chakraborty, A. K.; Ko, T.; Lee, C.; Lee, W. I. Heterojunction of $FeTiO_3$ nanodisc and TiO_2 nanoparticle for a novel visible light photocatalyst. *J. Phys. Chem. C* **2009**, *113*, 19179.

(23) Westmoreland, P. R.; Harrision, D. P. Evaluation of candidate solids for high-temperature desulfurization of low-BTU gases. *Environ. Sci. Technol.* **1976**, *10*, 659.

(24) Gogate, P. R.; Pandit, A. B. Engineering design methods for cavitation reactors II: Hydrodynamic Cavitation. *AIChE J.* **2000**, *46*, 1641.

(25) Tullis, J. P. Choking and supercavitating valves. *J. Hydraulics Div.* **1971**, *97*, 1931.

(26) Goel, M.; Hongqiang, H.; Mujumdar, A. S.; Ray, M. B. Sonochemical decomposition of volatile and non-volatile organic compounds—A comparative study. *Water Res.* **2004**, *38*, 4247.

(27) Lin, J. G.; Ma, Y. S. Magnitude of effect of reaction parameters on 2-chlorophenol decomposition by ultrasonic process. *J. Hazard. Mater.* **1999**, *66*, 291.

(28) Ince, N. H.; Guyer, G. T. Impacts of pH and molecular structure on ultrasonic degradation of azo dyes. *Ultrasonics* **2004**, *42*, 591.

(29) Teo, K. C.; Xu, Y.; Yang, C. Sonochemical degradation for toxic halogenated organic compounds. *Ultrason. Sonochem.* **2001**, *8*, 241.

(30) Chen, J. R.; Xu, X. W.; Lee, A. S.; Yen, T. F. A feasibility study of dechlorination of chloroform in water by ultrasound in the presence of hydrogen peroxide. *Environ. Technol.* **1990**, *11*, 829.

(31) Pandit, A. B.; Gogate, P. R.; Mujumdar, S. Ultrasonic degradation of 2:4:6 trichlorophenol in the presence of TiO_2 catalyst. *Ultrason. Sonochem.* **2001**, *8*, 227.

(32) Ambulgekar, G. V.; Samant, S. D.; Pandit, A. B. Oxidation of alkylarenes using aqueous potassium permanganate under cavitation: Comparison of acoustic and hydrodynamic cavitation. *Ultrason. Sonochem.* **2005**, *12*, 85.

(33) Senthilkumar, P.; Sivakumar, M.; Pandit, A. B. Experimental quantification of chemical effects of hydrodynamic cavitation. *Chem. Eng. Sci.* **2000**, *55*, 1633.

(34) Gogate, P. R.; Pandit, A. B. A review of imperative technologies for wastewater treatment I: Oxidation technologies at ambient conditions. *Adv. Env. Res.* **2004**, *8*, 501.

(35) Sivakumar, M.; Pandit, A. B. Wastewater treatment: A novel energy efficient hydrodynamic cavitational technique. *Ultrason. Sonochem.* **2002**, *9*, 123.

(36) Hung, H. M.; Hoffmann, M. R. Kinetics and mechanism of sonolytic degradation of chlorinated hydrocarbons: frequency effects. *J. Phys. Chem. A* **1999**, *103*, 2734.

(37) Petrier, C.; Lamy, M. F.; Francony, A.; Benachene, A.; David, B.; Renaudin, V.; Gondrexon, N. Sonochemical degradation of phenol in dilute aqueous solutions: Comparison of the reaction rates at 20 and 487 kHz *J. Phys. Chem.* **1994**, *98*, 10514.